Chaperone-Aided in Vitro Renaturation of an Engineered E1 Envelope Protein for Detection of Anti-Rubella Virus IgG Antibodies

Christian Scholz,*,‡ Laurence Thirault,‡ Peter Schaarschmidt,‡ Toralf Zarnt,‡ Elke Faatz,‡ Alfred Michael Engel,‡ Barbara Upmeier,‡ Ralf Bollhagen,‡ Barbara Eckert,§ and Franz Xaver Schmid§

Roche Diagnostics GmbH, Nonnenwald 2, D-82377 Penzberg, Germany, and Laboratorium für Biochemie, Universität Bayreuth, D-95440 Bayreuth, Germany

Received December 13, 2007; Revised Manuscript Received February 13, 2008

ABSTRACT: The envelope glycoproteins of Rubella virus, E1 and E2, mediate cell tropism, and E1 in particular plays a pivotal role in the fusion of the virus with the endosomal membrane. Both are the prime targets of the humoral immune response. Recombinant variants of the E1 ectodomain as well as E1 antigen preparations from virus lysates are commonly used to detect anti-Rubella immunoglobulins in human sera. Hitherto, recombinant E1 for diagnostic applications has been produced chiefly in eukaryotic expression systems. Here, we report the high-yield overproduction of an engineered E1 ectodomain in the *Escherichia coli* cytosol and its simple and convenient renaturation into a highly soluble and immunoreactive conformation. C-Terminal fusion to one or two units of the *E. coli* chaperone SlyD enhances expression, facilitates in vitro refolding, and improves the overall solubility of Rubella E1. As part of this fusion protein, the E1 ectodomain fragment of residues 201–432 adopts an immunoreactive fold, providing a promising tool for the sensitive and specific detection of anti-E1 IgG in Rubella serology. Two disulfide bonds in the membrane-adjacent part of the E1 ectodomain are sufficient to generate conformations with a high and specific antigenicity. The covalently attached chaperone modules do not impair antibody recognition and binding of Rubella E1 when assessed in a heterogeneous immunoassay. SlyD and related folding helpers are apparently generic tools for the expression and refolding of otherwise unavailable proteins of diagnostic or medical importance.

Rubella virus is the only member of the *Rubivirus* genus within the Togaviridae family. The small enveloped (+) RNA virus is a human pathogen and causes a mild, self-limiting childhood disease (German Measles or Rubella) characterized by rash, lymphadenopathy, and low-grade fever. When acquired in the first trimester of pregnancy, however, it may cause stillbirth, spontaneous abortion, or several anomalies associated with the congenital Rubella syndrome (*1*). The characteristic triad of congenital Rubella syndrome includes cataracts, heart defects, and deafness of the fetus. It necessitates Rubella vaccination programs and surveillance of the immune status of women in child-bearing age (*2, 3*).

The structural proteins of the Rubella virus originate from a single 110 kDa polypeptide precursor, which is proteolytically cleaved to yield capsid protein C and envelope proteins E2 and E1 (*4, 5*). E2 and E1 are glycosylated; they form noncovalent heterodimers at the surface of the virion (*6–9*) and are the preferred targets of the humoral immune response (*10, 11*). The membrane-anchored ectodomain of the E1 protein, in particular, is immunodominant, and antibodies against E1 are abundant in sera from Rubella-infected individuals (*12, 13*). Depending on the format of the respective immunoassay, E1 antigen variants have to fulfill different requirements. In a double-antigen sandwich (DAGS)[1] or bridge immunoassay, soluble antigens with low epitope density are mandatory for the specific detection of anti-Rubella IgG and for the determination of the concomitant immune status.

Initially, soluble fragments of E1 to be used as antigens for immunoassays were isolated from the supernatant of infected Baby hamster kidney (BHK-21) (*14*) or Vero cells (*15*). Later, various expression and secretion systems were developed with the aim of producing soluble and immunoreactive versions of E1 in eukaryotic hosts (*16, 17*). A glycosylated and soluble form of full-length E1 could be produced in baculovirus-infected *Spodoptera frugiperda*

* To whom correspondence should be addressed: Roche Diagnostics GmbH, Dept. DXR-IR, Nonnenwald 2, D-82377 Penzberg, Germany. Phone: ++49-8856-603878. Fax: ++49-8856-60793878. E-mail: christian.scholz@roche.com.

‡ Roche Diagnostics GmbH.

§ Universität Bayreuth.

[1] Abbreviations: SlyD, product of the *slyD* (sensitive to lysis D) gene; SlyD*, 1–165 fragment of SlyD; IF domain, insert-in-flap domain of SlyD; FkpA, FK506 binding protein A, periplasmic *Escherichia coli* chaperone; PPIase, peptidyl-prolyl *cis*/*trans* isomerase; IMAC, immobilized metal affinity chromatography; GdmCl, guanidinium chloride; Ni-NTA, nickel nitrilotriacetate; GSH and GSSG, reduced and oxidized forms of glutathione, respectively; DTNB (Ellman's reagent), 5,5′-dithiobis(2-nitrobenzoic acid); FPLC, fast protein liquid chromatography; CD, circular dichroism; ELISA, enzyme-linked immunosorbent assay; DAGS, double-antigen sandwich; IgG, immunoglobulin G; E1 and E2, transmembrane glycoproteins from Rubella virus; HIV-1, human immunodeficiency virus type 1; HTLV, human T-cell lymphotropic virus; gp41, gp36, and gp21, 41, 36, and 21 kDa transmembrane glycoproteins from HIV-1, HIV-2, and HTLV, respectively. ELECSYS and COMPLETE are trademarks of Roche.

10.1021/bi702435v CCC: $40.75
Published on Web 03/11/2008

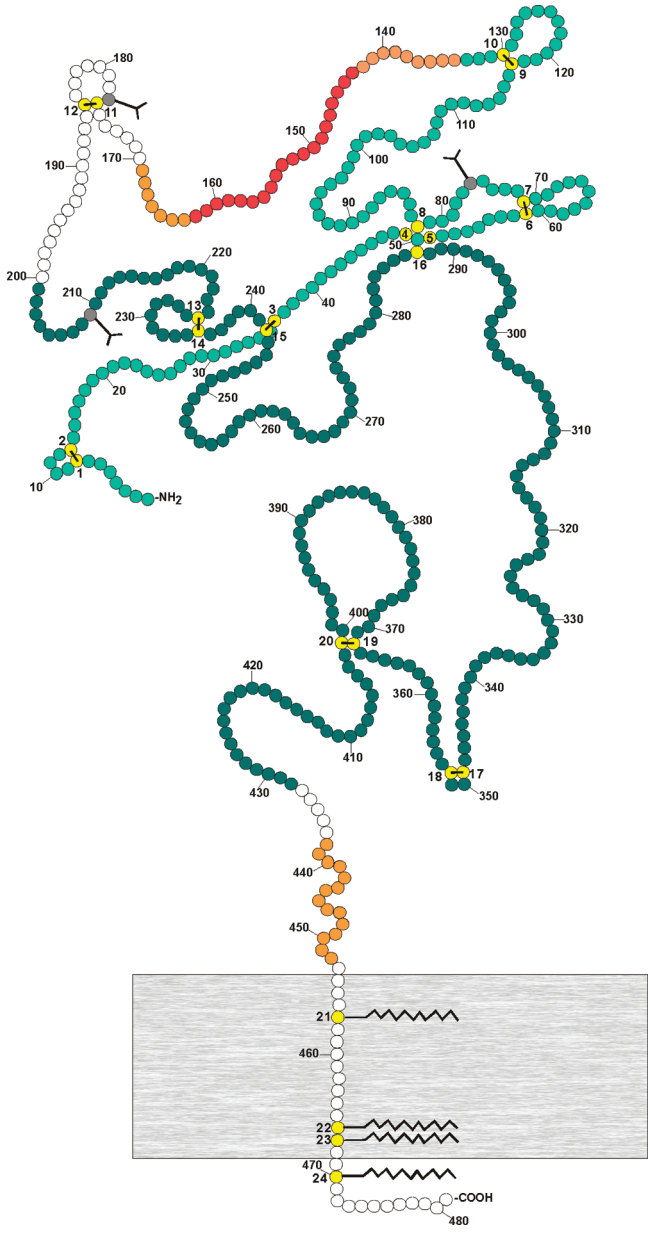

FIGURE 1: Topology scheme of the membrane-anchored Rubella E1 protein adapted from Gros et al. (*25*). The 24 cysteine residues are colored yellow and numbered contiguously; the three N-glycosylation sites of mature viral E1 are colored gray and marked with a Y. Disulfide pairings as assigned by the Wengler group (*25*) are indicated by black bars. Aggregation-promoting segments are colored orange (modestly aggregation-prone) and red (strongly aggregation-prone). The N fragment of residues 1–133 (bright green) and the C fragment of residues 201–432 (dark green) were expressed in fusion with tandem SlyD* in *E. coli* and refolded from inclusion bodies to yield soluble monomers.

(*18, 19*) and CHO cells (*20*) and, most recently, in *Pichia pastoris* (*21*). The expression of Rubella-like particles in BHK cells (*22*) and in a stably transfected CHO cell line (*23, 24*) yielded Rubella antigens suitable for diagnostic purposes. These Rubella-like particles are noninfectious, ill-defined agglomerates of the covalently linked Rubella proteins C, E2, and E1 and are useful for detecting immunoglobulins of the M and G type.

The Rubella E1 protein, also termed Rubella hemagglutinin (Figure 1), presumably consists of a large ectodomain (residues 1–452), followed by a single transmembrane helix (residues 453–468) and a short cytoplasmic tail (residues 469–481). Residues 438–452, which immediately precede the transmembrane region, probably form also a helix (*25*). The ectodomain of E1 bears 20 cysteine residues, which are engaged in 10 disulfide bonds. The C(1)−C(2), C(3)−C(15), C(6)−C(7), C(9)−C(10), C(11)−C(12), C(13)−C(14), C(17)−C(18), and C(19)−C(20) cysteine pairs could be confirmed with certainty, whereas the pairing of cysteine residues C(4), C(5), C(8), and C(16) remains ambiguous (*25*). The ectodomain is glycosylated at the three asparagines at positions 76, 177, and 209. It is unclear whether these carbohydrate chains are essential for the function and antigenicity of E1 (*26–28*).

Nonglycosylated forms of E1 could, in principle, be produced much more efficiently in a prokaryotic host. In an early attempt, a full-length and a truncated version (207–353) of Rubella E1 were fused to protein A from *Staphylococcus aureus* and produced in *E. coli* (*29*). These fusion proteins were active as antigens but only of limited value for the specific detection of anti-E1 antibodies. In general, variants of E1 from prokaryotic hosts exhibited a strong tendency to aggregate, possibly because they are unglycosylated, or because they are incorrectly disulfide bonded. In fusion with glutathione *S*-transferase, only small fragments of E1 comprising as little as 75 or 44 amino acid residues could be expressed in a soluble and functional form (*30, 31*). Larger E1 fragments encompassing 82 or 171 amino acid residues could be obtained when fused to both RecA and β-galactosidase (*32*).

The oxidative refolding of large cysteine-rich proteins such as E1 is very difficult, because misfolded intermediates with the wrong disulfides, which are trapped during refolding, have a very strong tendency to aggregate. Therefore, many efforts concentrated on finding contiguous B-cell epitopes along the E1 polypeptide chain (*13, 33, 34*) and to use corresponding short soluble peptides as antigens in immunoassays (*35–38*). Antibodies generally show modest affinities toward small peptide antigens, and therefore, producing stable and soluble fragments of E1 with a high antigenicity and in large amounts remains a major goal, ideally by the massive production as inclusion bodies in a prokaryotic host, followed by a robust renaturation procedure.

Recently, we found that the covalent fusion with the chaperone SlyD or FkpA maintains aggregation-prone proteins or protein fragments, such as the gp41 ectodomain from HIV-1, in a soluble and functional form (*39*). SlyD is located in the cytosol of *E. coli*, and FkpA resides in the periplasm. Both combine prolyl isomerase and chaperone activities and are probably involved in protein folding in vivo (*40–44*). They bind reversibly to unfolded and partially folded polypeptide segments and assist protein folding in an ATP-independent fashion. The chaperone function of FkpA has been confined to the dimerizing N domain (*44, 45*), whereas the polypeptide binding site of SlyD resides in its IF (insert in flap) domain (*46*).

To develop a soluble monomeric form of E1 with strong and specific binding to anti-Rubella antibodies, we fused two SlyD* molecules in tandem to the amino terminus of E1 fragments of variable length. SlyD* is the fragment of residues 1–165 of SlyD, which lacks the cysteine-rich C-terminal tail. It is devoid of cysteine residues and cannot form incorrect disulfide bonds with the target protein. SlyD* folds and unfolds reversibly, and it forms soluble and

dynamic complexes with the proteins to which it is attached (*39, 42*).

Hitherto, robust and functional forms of the E1 ectodomain could not be obtained from prokaryotic hosts, probably because the protein is large (452 residues) and because the 20 cysteine residues can form a vast array of abortive species with incorrect disulfide bonds. To tackle these problems, we used a divide-and-conquer strategy. We started by replacing all cysteine residues of E1 with alanine. Then, a panel of fragments with successive deletions from the termini was created to identify those fragments that are highly soluble in the absence of disulfide bonds. In the second step, the native disulfide bonds were transferred back into the length-optimized fragments, first individually and then in combinations of two or three disulfides. Ultimately, optimized C-terminal fragments of E1 with 232 amino acids and two or three disulfide bonds could be identified. They were stable, soluble, and well suited for the specific detection of anti-E1 IgG in Rubella-positive human sera.

MATERIALS AND METHODS

Materials and Reagents. GdmCl (A-grade) was purchased from NIGU (Waldkraiburg, Germany). Complete EDTA-free protease inhibitor tablets, L-lysine, imidazole, and EDTA were from Roche Diagnostics GmbH (Mannheim, Germany), DTNB (Ellman's reagent) was from Sigma-Aldrich (St. Louis, MO), all other chemicals were analytical-grade and from Merck (Darmstadt, Germany). Ultrafiltration membranes (YM10 and YM30) were purchased from Amicon (Danvers, MA), and microdialysis membranes (VS, 0.025 μm) and ultrafiltration units (biomax ultrafree filter devices) were from Millipore (Bedford, MA). Cellulose nitrate and cellulose acetate membranes (1.2, 0.45, and 0.2 μm pore size) for the filtration of crude lysates were from Sartorius (Göttingen, Germany).

Cloning of Expression Cassettes. The sequence of the E1 precursor protein from Rubella strain Therien (*47*) was retrieved from the SwissProt database (accession number P07566). A synthetic gene encoding Rubella E1 (amino acids 1–432) was purchased from Medigenomix (Martinsried, Germany) and cloned into a pET24 expression vector (Novagen, Madison, WI). The codon usage was optimized for expression in *E. coli* host cells. The expression cassettes for the various SlyD* fusion proteins were designed essentially as described previously (*39*). To prevent homologous recombination within the tandem cassette, nucleotide sequences encoding repetitive elements were degenerated. QuikChange (Stratagene, La Jolla, CA) and standard PCR techniques were used to generate truncation and extension variants or restriction sites. All recombinant E1 fusion polypeptide variants contained a C-terminal hexahistidine tag to facilitate Ni-NTA-assisted purification and refolding.

Expression, Purification, and Refolding of SlyD Variants and Fusion Proteins.* All E1 variants were purified and refolded by using virtually identical protocols. *E. coli* BL21(DE3) cells harboring the particular pET24a expression plasmid were grown at 37 °C in LB medium with kanamycin (30 μg/mL) to an OD_{600} of 1.5, and cytosolic overexpression was induced by adding 1 mM isopropyl β-D-thiogalactoside. Three hours after induction, cells were harvested by centrifugation (20 min at 5000*g*), frozen, and stored at −20 °C. For cell lysis, the frozen pellet was resuspended in chilled 50 mM sodium phosphate (pH 8.0), 7.0 M GdmCl, and 5 mM imidazole, and the suspension was stirred for 2 h on ice to complete cell lysis. After centrifugation and filtration (cellulose nitrate membrane, 0.45 and 0.2 μm), the lysate was applied to a Ni-NTA column equilibrated with the lysis buffer, including 5.0 mM TCEP. In the subsequent washing step, the imidazole concentration was increased to 10 mM [in 50 mM sodium phosphate (pH 8.0), 7.0 M GdmCl, and 5.0 mM TCEP] and at least 15–20 volumes of the washing buffer was applied. Then, the GdmCl solution was replaced with 50 mM sodium phosphate (pH 8.0), 100 mM NaCl, 10 mM imidazole, and 5.0 mM TCEP to induce conformational refolding of the matrix-bound fusion polypeptide. To prevent reactivation of copurifying proteases, a protease inhibitor cocktail (Complete EDTA-free, Roche) was included in the refolding buffer. A total of 15–20 column volumes of refolding buffer was applied to the mixture overnight. Then, both TCEP and the Complete EDTA-free inhibitor cocktail were removed by washing with 10 column volumes of 50 mM sodium phosphate (pH 8.0), 100 mM NaCl, and 10 mM imidazole. In the last washing step, the imidazole concentration was increased to 40 mM (10 column volumes) to remove tenacious contaminants. The native protein was then eluted with 250 mM imidazole in the same buffer. Protein-containing fractions were assessed for purity by Tricine SDS−PAGE (*48*) and pooled. Subsequently, the proteins were subjected to size-exclusion chromatography (Superdex HiLoad, Amersham Pharmacia) using potassium phosphate as the buffer system [50 mM potassium phosphate (pH 7.5), 100 mM KCl, and 1 mM EDTA]. Finally, the protein-containing fractions were pooled and concentrated in an Amicon cell (YM10). Since the E1 variant (201–432) without a SlyD* fusion partner spontaneously aggregated upon matrix-coupled refolding and imidazole elution, the purification protocol was slightly modified: after conformational and oxidative refolding coupled to the Ni-NTA matrix, the disulfide-bonded protein was again unfolded with GdmCl and eluted in an unfolded form when the pH was lowered to 6.0.

Spectroscopic Measurements. Protein concentration measurements were performed with a Uvikon XL double-beam spectrophotometer. The molar extinction coefficients (ϵ_{280}) for the fusion proteins were calculated using the method of Pace (*49*).

Near-UV and far-UV CD spectra were recorded with a Jasco-720 spectropolarimeter with a thermostated cell holder (20 °C). For near-UV CD spectra, the buffer included 50 mM potassium phosphate (pH 7.5), 100 mM KCl, and 1 mM EDTA. The path length was 0.5 or 1.0 cm, and the protein concentration was 100 μM. The bandwidth was 1 nm, the scanning speed 20 nm/min at a resolution of 0.5 nm, and the response 2 s. For far-UV CD spectra, the buffer included 10 mM potassium phosphate (pH 7.0) and 100 mM KF in a 0.1 cm cuvette at a protein concentration of 1.5 μM. To improve the signal-to-noise ratio, spectra were measured nine times and averaged.

Rubella E1 Aggregation Assay. The assay was performed in a thermostated cuvette holder under gentle stirring essentially according to the citrate synthase assay outlined by Buchner et al. (*50*). E1 variants bearing zero, one, and two SlyD* units were unfolded at 35 °C in 6.0 M GdmCl,

20 mM DTT, and 50 mM potassium phosphate (pH 7.0) for 1 h and then diluted 135-fold to a final concentration of 0.1 μM in 44 mM GdmCl, 50 mM KCl, 10 mM DTT, and 50 mM potassium phosphate (pH 7.0) at 35 °C. The elevated temperature of 35 °C was chosen to accelerate the aggregation process of E1 (201–432). The reducing refolding environment was chosen so that aggregation due to covalent disulfide adduct formation by the cysteine thiols could be ruled out. Spontaneous aggregation was monitored by the increase in light scattering at 340 nm (excitation and emission bandpass of 5 nm) in a Hitachi F4010 fluorescence spectrometer.

Coupling of Biotin and Ruthenium Moieties to the Fusion Proteins. The lysine ϵ-amino groups of the Rubella E1 fusion polypeptides were modified at protein concentrations of ~15 mg/mL with *N*-hydroxysuccinimide-activated biotin and ruthenium labels, respectively. The label:protein molar ratio varied from 2:1 to 5:1, depending on the respective fusion protein. The reaction buffer included 150 mM potassium phosphate (pH 8.0), 50 mM KCl, and 1 mM EDTA. The reaction was carried out at room temperature for 15 min and stopped by adding buffered L-lysine to a final concentration of 10 mM. To prevent hydrolytic inactivation of the labels, the respective stock solutions were prepared in dried DMSO (seccosolv quality, Merck). DMSO concentrations of up to 15% in the reaction buffer were tolerated well by all fusion proteins that were studied. After the coupling reaction, unreacted free label was removed by passing the crude protein conjugate over a gel filtration column (Superdex 200 HiLoad).

Immunological Reactivity of the Ectodomain Fusion Proteins. The E1 variants were used to detect anti-E1 antibodies, which abundantly occur in Rubella-positive human sera. The immunological reactivity was assessed in an automated Elecsys 2010 analyzer using the double-antigen sandwich format. Signal detection in Elecsys 2010 instruments is based on electrochemiluminescence. The biotin conjugate (i.e., the capture antigen) is immobilized on the surface of a streptavidin-coated magnetic bead, whereas the detection antigen bears a complexed ruthenium cation (switching between the 2+ and 3+ redox states) as the signaling moiety. In the presence of a specific (i.e., anti-Rubella E1) immunoglobulin analyte, the chromogenic ruthenium complex is bridged to the solid phase and emits light at 620 nm after excitation at a platinum electrode. The photomultiplier signal readout is in arbitrary light units.

All SlyD*−SlyD*−E1 fusion proteins were assessed for their reactivity against anti-Rubella positive sera at concentrations of ~500 ng/mL for both the biotinylated form and the ruthenylated form.

At least seven negative sera were used as controls. In all measurements, a chemically polymerized SlyD*−SlyD* variant was implemented in the reaction buffer as an anti-interference substance to prevent immunological cross reactions via the chaperone fusion unit.

RESULTS

Expression of a Rubella E1 Ectodomain Fused to SlyD in E. coli.* In a first attempt to improve the production of soluble and functional variants of the E1 protein, we fused two SlyD* modules in tandem to the N-terminus of fragment 1–432 of E1. This fragment contains essentially the ectodomain but lacks the C-terminal helix, the transmembrane helix, and the cytosolic tail of E1 (Figures 1 and 2). In this version of E1, all cysteine residues were mutated to alanine to prevent disulfide formation. The fusion protein was expressed well in *E. coli* BL21/DE3, unlike the E1 ectodomain without the two SlyD* modules, but most of the fusion protein was found in inclusion bodies. Solubilization in 7.0 M GdmCl, matrix-coupled refolding, and size-exclusion chromatography were performed as described in Materials and Methods. All proteins of this study were C-terminally tagged with a hexahistidine sequence to enable Ni-NTA-coupled purification and refolding. After removal of the denaturant and elution by imidazole, the fusion protein remained soluble in 50 mM potassium phosphate (pH 7.5), 100 mM KCl, and 1 mM EDTA at concentrations up to 5 mg/mL. In size-exclusion chromatography on a Superdex 200 column, the fusion protein eluted in the void volume, suggesting that it either was in an extended conformation or formed soluble oligomers.

Identification of Soluble and Functional Fragments of the Rubella E1 Ectodomain. To identify soluble monomeric forms of the E1 ectodomain, we constructed fragments of variable length (Figure 3). All of them were expressed in fusion with two SlyD* modules in tandem at the amino terminus. Initially, we split the E1 ectodomain between Asp314 and Pro315 into a large N fragment, E1 (1–314), and a small C fragment, E1 (315–432). We chose these boundaries since Asp−Pro peptide bonds are labile at acidic to neutral pH and tend to hydrolyze spontaneously (*51*). After lysis, binding to an IMAC column in 7.0 M GdmCl, and renaturation on the column, the large N fragment (1–314) was eluted as a soluble protein, but as the full-length ectodomain (1–432), it eluted in the void volume during size-exclusion chromatography (Figure 4B). The C fragment 315–432 (51.7 kDa) could be solubilized by the same procedure, and it eluted from the Superdex 200 column with an apparent molecular mass of ~110 kDa (Figure 4A). Apparently, the tandem fusion with SlyD* kept the E1 fragments soluble, but it could not prevent oligomerization of the large N fragment (1–314).

Dissection of the C-Terminal Part of the Rubella E1 Ectodomain. In the following, we used the short C fragment (315–432) as a starting sequence to identify larger versions of E1 that retain a high overall solubility and do not form higher-order oligomers. Toward this end, fragment 315–432 was extended stepwise in both directions. The C-terminal expansion by residues 433–452, which adds the putative C-terminal helix of the ectodomain, led to a strong increase in the tendency to aggregate, and therefore, Val432 was kept as the C-terminal residue for all subsequent versions of E1 (cf. Figure 3).

The two variants, 260–432 (57.6 kDa) and 201–432 (64.1 kDa), exhibited excellent solubility and eluted with apparent molecular masses of 120 and 130 kDa, respectively, in FPLC analysis (Figure 4A). These elution patterns are reminiscent of the carrier module SlyD*, which also eluted at the position of an apparent dimer during Superdex 200 gel filtration, although analytical ultracentrifugation had unambiguously shown that SlyD* is monomeric (*42*). This discrepancy is due to the elongated shape of SlyD*. Presumably, the same holds for the SlyD*−SlyD*−E1 fusion polypeptides, which

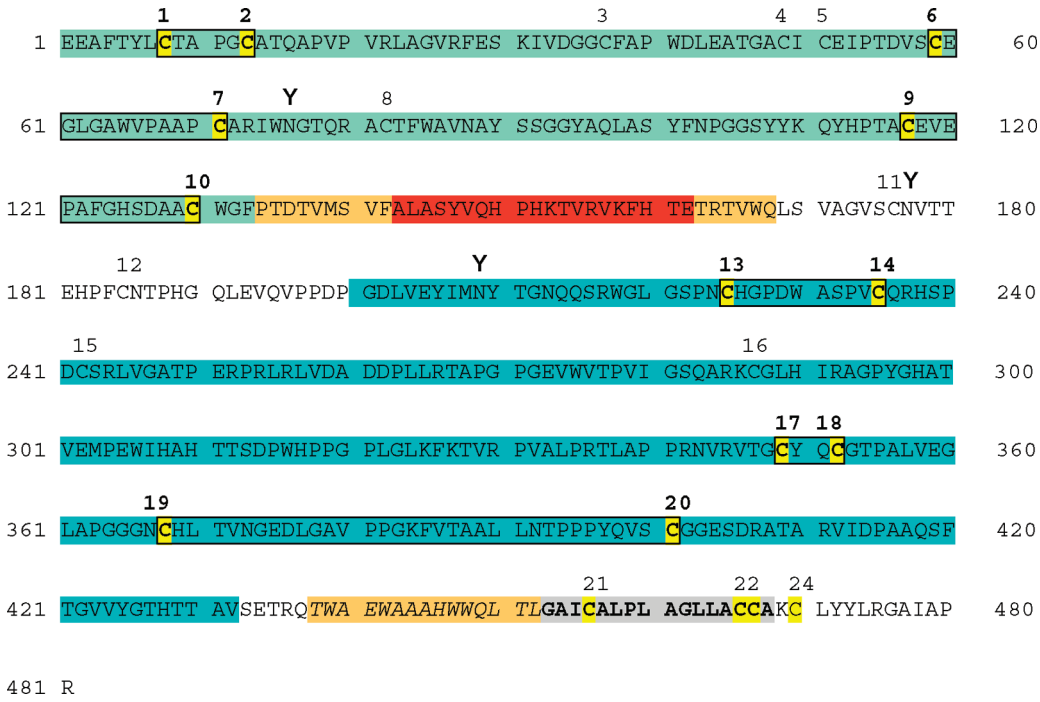

FIGURE 2: Amino acid sequence of the E1 envelope protein from the Rubella Therien strain (*47*). Mature E1 comprises 481 residues after processing of the precursor polypeptide. A putative transmembrane segment of residues 453–468 (bold letters on a gray background) anchors the E1 ectodomain (1–452) to the viral surface. The adjacent putative helical segment of residues 438–452 is italicized. The twenty-four cysteine residues within E1 are colored yellow and numbered contiguously as described by Gros et al. (*25*). The disulfide-bonded loops investigated in this study are boxed, and the corresponding cysteine residues (1, 2, 6, 7, 9, 10, 13, 14, and 17−20) are printed in bold. The two large E1 fragments that were soluble monomers in fusion with tandem SlyD* are highlighted: the E1 N fragment (1–133) colored bright green and the E1 C fragment (201–432) dark green. Aggregation-promoting segments are colored orange (modestly aggregation prone) and red (strongly aggregation prone). The three asparagines that are glycosylated in mature viral E1 are marked with a Y.

are extended rather than globular. It is therefore likely that E1 variants 260–432 and 201–432 are indeed monomeric. A further extension to include residues 143–200 (yielding fragment 143–432) again led to high-molecular mass associates.

In summary, these studies indicated that C-terminal fragment 201–432 of the E1 ectodomain remained soluble in a presumably monomeric form, but that further extension to include the region of residues 143–200 led to high-molecular mass associates. To identify more precisely the chain region that promotes this undesired aggregation, we constructed, again in tandem fusion with SlyD*, a series of fragments with closely spaced N-termini at positions Arg156, Thr163, and Leu169. Immediately after solubilization, these fragments eluted within the separation range of the gel filtration column. However, when incubated at 25 °C for more than 12 h and at protein concentrations higher than 10 mg/mL, fragments 156–432 and 163–432 tended to aggregate and eluted in the void volume during gel filtration. Fragment 169–432 remained soluble under these conditions (Figure 4A) but was transformed into a high-molecular mass form when the temperature was increased to 42 °C. This indicates that all three N-terminal extensions of fragment 201–432 strengthened the tendency to form high-molecular mass associates. Apparently, fragment 201–432 is the largest C fragment of E1 that remains soluble for an extended time, even in the absence of the disulfide bonds.

Dissection of the N-Terminal Part of the Rubella E1 Ectodomain. The large 1–314 N-terminal fragment aggregated rapidly. To identify shorter versions with possibly improved solubility, shortened N fragments 1–200, 1–142, 1–104, and 1–55 were constructed and fused with two SlyD* modules. The largest fragment, E1 (1–200), overlapped with the longest C-terminal fragments in the region of residues 143–200 (Figure 3), and like these fragments, it exhibited a strong tendency to aggregate. This suggests that the presence of the region of residues 143–200 substantially decreases the solubility. The shorter N-terminal fragments 1–55, 1–104, and 1–142 all eluted as apparent dimers after matrix-coupled refolding (Figure 4B). After an overnight incubation at 42 °C (at a protein concentration of ~5 mg/mL), the short 1–55 and 1–104 variants remained soluble and only the 1–142 variant aggregated.

The importance of the region of residues 104–142 for solubility was further mapped by producing fragments 1–117 and 1–133 in tandem fusion with two SlyD* modules. Both fragments were highly soluble, even at 42 °C and at concentrations up to 10 mg/mL. In summary, the truncation and extension experiments (Figure 3) show that N-terminal fragment 1–133 and C-terminal fragment 201–432 (in tandem fusion with the PPIase chaperone SlyD*) can be produced in a robust and soluble form, even in the absence of the disulfide bonds. The experiments also revealed that the region of residues 140–170 probably harbors an aggregation or oligomerization motif, since all fragments that extended into this region showed a markedly decreased solubility. In fact, the segment between Tyr137 and Phe 149 of the E1 ectodomain shows the highest local hydrophobicity, and a further region of high hydrophobicity extends from Val166 to Val174 (*52, 53*).

Restoration of Disulfide Bonds in the N-Terminal Fragment of E1. In spite of their good solubility, all the

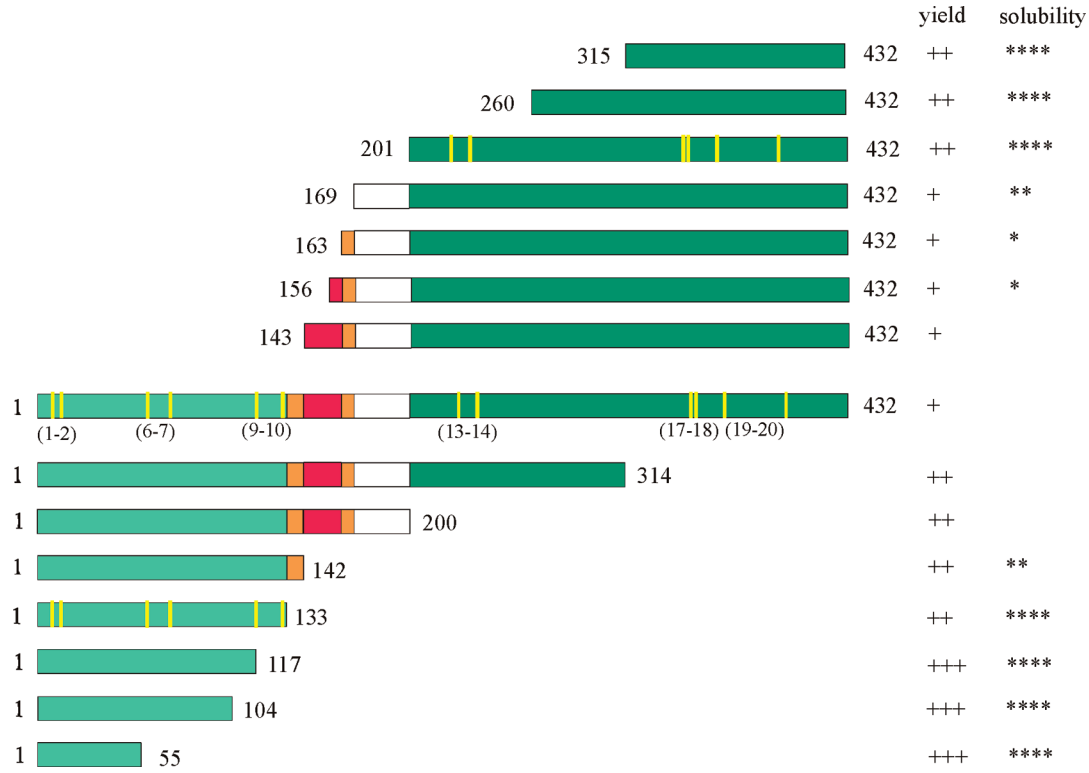

FIGURE 3: Truncation and extension scheme of Rubella E1. Starting with a large N fragment (1–314) and a smaller C fragment (315–432) devoid of cysteine residues, we expressed E1 constructs with different lengths as SlyD*−SlyD* fusion proteins. The disulfide pairs combined in the length-optimized E1 fragments are marked with yellow bars and numbered contiguously as described by Gros et al. (*25*). A putative oligomerization motif is colored orange (modestly aggregation prone) and red (strongly aggregation prone). The expression yield and solubility of each construct are estimated with a plus and asterisk, respectively. In a rough approximation, the yield (in milligrams of protein per gram of cell wet weight) is rated + (1–5 mg/g), ++ (5–10 mg/g), or +++ (>10 mg/g). The solubility of monomeric E1 (in milligrams per milliliter, protein in phosphate buffer at ambient temperature) is rated * (<5 mg/mL), ** (5–10 mg/mL), *** (10–20 mg/mL), or **** (>20 mg/mL).

aforementioned N- and C-terminal fragments were essentially inactive; i.e., they did barely react in Rubella immunoassays, presumably because they were unable to fold into a nativelike antigenic conformation in the absence of the disulfide bonds. Therefore, in the following, we investigate which disulfide bonds are required to convey a high immunological reactivity to these fragments.

Most of the disulfide bonds in the E1 ectodomain have been identified (*25*), and we used these assignments to reintroduce the native disulfide bonds, one at a time, into the length-optimized soluble E1 fragments. Then, all these single-disulfide-bond fragments were assessed for their immunological reactivities in a DAGS format with human anti-Rubella sera.

The matrix-assisted purification and refolding method was adapted to allow disulfide formation on the column. First, the bound protein was washed with 7.0 M GdmCl in the presence of 5 mM TCEP. In this step, both correct and incorrect disulfide bonds are reduced to free cysteines. TCEP was used, since it is compatible with IMAC and does not reduce the Ni-NTA groups. Subsequently, the reduced protein was refolded in the presence of 5 mM TCEP by omitting the denaturant from the buffer. In this step, the protein is supposed to adopt a nativelike conformation, which brings the matching cysteines into the proximity of each other. Then, the oxidation of the matrix-bound protein was induced by omitting TCEP from the refolding buffer. This uncoupling of conformational and oxidative in vitro refolding led to a high yield of nativelike disulfide-bonded molecules. In nonreducing Tricine SDS−PAGE (*48*), all single-disulfide variants migrated as homogeneous bands, and there was no evidence for disulfide-bonded oligomers. Free thiol groups could not be detected by Ellman's assay (*54*), indicating that the disulfide bonds were fully formed.

First, we focused on N fragment 1–133 and individually reintroduced the C(1)−C(2), C(6)−C(7), and C(9)−C(10) cysteine pairs. This did not lead to immunological reactivity. In the next step, we combined two disulfide bonds in all possible combinations, but this did not improve the immunoreactivity either (Table 1). The same result was found for the variant with all three disulfide bonds. The antigenic properties of N fragment 1–133 of E1 could thus not be substantially improved by reintroduction of one, two, or three of the disulfide bonds, and therefore, this fragment was not employed in the further optimizations. Our results are in line with peptide-based studies, which showed a rather poor reactivity of antibodies toward the N-terminal region of E1 (*33*).

Restoration of Disulfide Bonds in the C-Terminal Fragment of E1. Several IgG binding sites and four neutralizing epitopes have been mapped to the region of residues 202−285 of E1 (*32, 33, 36, 55*). C fragment 201–432 contains three nonoverlapping disulfide bonds, C(13)−C(14), C(17)−C(18), and C(19)−C(20) (*25*). The C(13)−C(14) bond closes a short loop of nine residues, including a tryptophan (W230), and the C(19)−C(20) bond closes a rather large loop with 32 intervening residues (Figures 1 and 2). Cys349 and Cys352, which form the C(17)−C(18)

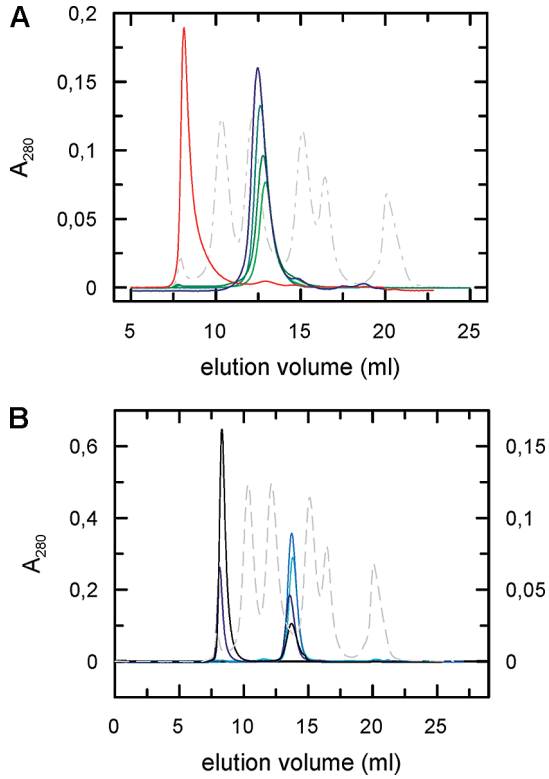

FIGURE 4: Analytical size-exclusion chromatography on a Superdex 200 HR 10/30 column of SlyD*−SlyD* fusion variants of Rubella E1. The E1 C fragments (300 μg) (A) and the E1 N fragments (400 μg) (B) were applied on the gel filtration column in a volume of 200 μL, and elution was monitored at 280 nm. As a reference, 100 μg of a molecular mass standard [β-galactosidase (465 kDa), sheep IgG (150 kDa), sheep IgG Fab fragment (50 kDa), horse myoglobin (17 kDa), and Gly-Tyr (0.238 kDa)] was applied in 100 μL (gray dashed line, right ordinate in panel B). The buffer included 50 mM potassium phosphate (pH 7.0), 100 mM KCl, and 1 mM EDTA. Shown are (A) the elution profiles of C fragments 315–432 (bright green line), 260–432 (dark green line), 201–432 (light blue line), 169–432 (dark blue line), and 143–432 (red line). In panel B, the elution profiles of N fragments 1–104 (light blue line), 1–133 (blue line), 1–142 (dark blue line), and 1–314 (black line) are depicted.

disulfide, are separated by two residues only, Y350 and Q351 (Figures 1 and 2). Cys-X-X-Cys motifs occur frequently in the active sites of disulfide oxidoreductases (*56*) and in metal ion binding sites.

To assess the role of the disulfide bonds in the antigenicity of the C-terminal fragment, we also first produced the three variants with a single disulfide each. Fused with a SlyD*−SlyD* pair, they were very well overproduced, with average yields of 5 mg of protein/g of cell wet weight. The three single-disulfide variants exhibited variable activities in immunoassays with anti-Rubella IgG-positive sera (Table 2). The variant with the C(13)−C(14) disulfide bond, in particular, discriminates well between Rubella-negative and Rubella-positive human sera. Molecules with a C(19)−C(20) or C(17)−C(18) disulfide reacted with several but not all of the positive sera. Thus, for the C-terminal fragments of E1, introducing single disulfide bonds basically generated immunological reactivity, probably by stabilizing conformational epitopes within the disulfide-fixed loops. The immunoreactivity of the single-disulfide E1 C fragments is, however, too low for a reliable DAGS immunoassay.

In two alternative constructs, the local C(17)−C(18) disulfide was combined either with the C(13)−C(14) disulfide or with the C(19)−C(20) disulfide. Multiple disulfide bond formation and isomerization of a Ni-NTA-coupled protein is not trivial, because cysteine oxidation is strongly catalyzed by transition metal ions like Ni^{2+}. We again followed the strategy for uncoupling conformational and oxidative refolding; i.e., we first induced conformational refolding while keeping the cysteine residues reduced and then induced disulfide bridging by omitting TCEP as the reducing agent. It turned out that air oxygen together with the Ni^{2+} ions of the column led to effective and correct disulfide bonding. The addition of GSH and GSSG in molar ratios ranging from 10:1 to 1:10 did not further increase the refolding yields. The fragment with the C(17)−C(18)/C(19)−C(20) disulfide combination exhibited an excellent

Table 1: Immunological Reactivities[a] of N-Terminal Rubella E1 (1–133) Variants[b] with Double-Disulfide-Bond Combinations

	C(1)−C(2), C(9)−C(10)	C(6)−C(7), C(9)−C(10)	C(1)−C(2), C(6)−C(7)
	Rubella-Negative Sera		
average counts	4559	4301	4838
	Rubella-Positive Sera		
relative signal			
BRK 01/2003_115	0.95	0.96	0.96
BRK 01/2003_116	1.02	1.06	1.03
BRK 01/2003_119	1.01	0.99	1.00
BRK 01/2003_123	1.05	1.09	1.16
BRK 01/2003_127	1.02	1.01	1.02
BRK 01/2003_130	0.96	0.95	0.97
BRK 01/2003_157	0.95	0.92	0.94
BRK 01/2003_159	0.96	0.96	0.98
BRK 01/2003_162	1.01	1.00	0.97
BRK 01/2003_166	1.02	1.00	1.02

[a] The immunoassays were performed by using an Elecsys 2010 analyzer as described in Materials and Methods. The relative signals are normalized relative to the average value obtained for seven Rubella-negative samples. The Rubella-positive sera were purchased from the Bavarian Red Cross, and the Rubella-negative controls were purchased from Trina International Bioreactives AG. [b] All E1 variants were soluble SlyD*−SlyD* fusion proteins, and their respective disulfide bond combinations are given.

Table 2: Immunological Reactivities[a] of C-Terminal Rubella E1 (201–432) Variants[b] with and without a Single Disulfide Bond

	C(13)−C(14)	C(17)−C(18)	C(19)−C(20)	no disulfide
	Rubella-Negative Sera			
average counts	2076	1453	2487	2076
	Rubella-Positive Sera			
relative signal				
BRK 01/2003_115	23.55	34.88	17.94	18.17
BRK 01/2003_116	17.09	7.96	5.83	4.37
BRK 01/2003_119	13.47	1.89	5.92	0.94
BRK 01/2003_123	10.30	5.72	6.66	4.10
BRK 01/2003_127	11.82	3.37	2.93	1.82
BRK 01/2003_130	12.81	2.37	1.58	1.46
BRK 01/2003_157	3.09	3.33	2.35	1.73
BRK 01/2003_159	2.31	1.79	1.14	0.91
BRK 01/2003_162	15.34	16.58	11.68	7.70
BRK 01/2003_166	7.12	2.96	1.64	1.44

[a] The immunoassays were performed by using an Elecsys 2010 analyzer as described in Materials and Methods. The relative signals are normalized relative to the average value obtained for seven Rubella-negative samples. The Rubella-positive sera were purchased from the Bavarian Red Cross, and the Rubella-negative controls were purchased from Trina International Bioreactives AG. [b] All E1 variants were soluble SlyD*−SlyD* fusion proteins, and their respective disulfide bonds are given.

Table 3: Immunological Reactivities[a] of C-Terminal Rubella E1 (201–432) Variants[b] with Double- and Triple-Disulfide-Bond Combinations

	C(17)−C(18) C(19)−C(20)	C(13)−C(14) C(17)−C(18)	C(13)−C(14) C(17)−C(18) C(19)−C(20)
	Rubella-Negative Sera		
average counts	2830	2072	4610
	Rubella-Positive Sera		
relative signal			
BRK 01/2003_115	22.77	42.92	22.98
BRK 01/2003_116	33.22	51.67	36.12
BRK 01/2003_119	44.22	89.58	45.90
BRK 01/2003_123	78.60	71.99	73.62
BRK 01/2003_127	37.56	42.14	37.83
BRK 01/2003_130	9.61	28.88	16.24
BRK 01/2003_157	17.87	20.23	16.49
BRK 01/2003_159	14.59	18.92	14.01
BRK 01/2003_162	31.25	53.29	31.06
BRK 01/2003_166	9.16	17.55	11.70

[a] The immunoassays were performed by using an Elecsys 2010 analyzer as described in Materials and Methods. The relative signals are normalized relative to the average value obtained for seven Rubella-negative samples. The Rubella-positive sera were purchased from the Bavarian Red Cross, and the Rubella-negative controls were purchased from Trina International Bioreactives AG. [b] All E1 variants were soluble SlyD*−SlyD* fusion proteins, and their respective disulfide bond combinations are given.

immunoreactivity, and it discriminated well between Rubella-positive and Rubella-negative human sera in the DAGS assays (Table 3). Remarkably, the signal-to-noise ratio was very high when compared to those of the single-disulfide forms, which exhibited much lower reactivity with the same sera (Table 2). Similarly, the fragment with the C(13)−C(14)/C(17)−C(18) combination exhibited a very high immunoreactivity (Table 3). Thus, the combination of the C(13)−C(14) disulfide or the C(19)−C(20) disulfide with the local C(17)−C(18) disulfide bond led to a strong increase in reactivity.

Finally, we combined all three disulfide bonds [C(13)−C(14), C(17)−C(18), and C(19)−C(20)] in a single variant of the C-terminal fragment. This variant could also be produced in large amounts. Comparable to the E1 constructs with the double-disulfide combinations, the E1 variant with three disulfide bonds exhibited less than 5% free thiols when assessed according to Ellman (*54*), and it migrated as a homogeneous band in Tricine SDS−PAGE (*48*).

The CD spectra of the E1 (201–432) fusion constructs with and without the three disulfide bonds are shown in Figure 5A. To obtain an estimate of the secondary structure of the E1 moiety of the fusion protein, we subtracted the CD spectra of two copies of SlyD (Figure 5B) from these spectra. The difference CD spectra are rather featureless and show pronounced minima below 200 nm for both fusion constructs (Figure 5C), indicating that the E1 parts of the fusion proteins are largely unfolded. The CD in this region is, however, significantly smaller for the construct with the disulfide bonds, indicating that the presence of the disulfide bonds leads to a decrease in the amount of unordered structure. In terms of its immunological reactivity, it was not significantly better than a combination of the variants with the two disulfide bonds (Table 3). Thus, the 201–432 fragments with two disulfide bonds and in fusion with two SlyD* modules represent the simplest forms of the Rubella E1 ectodomain

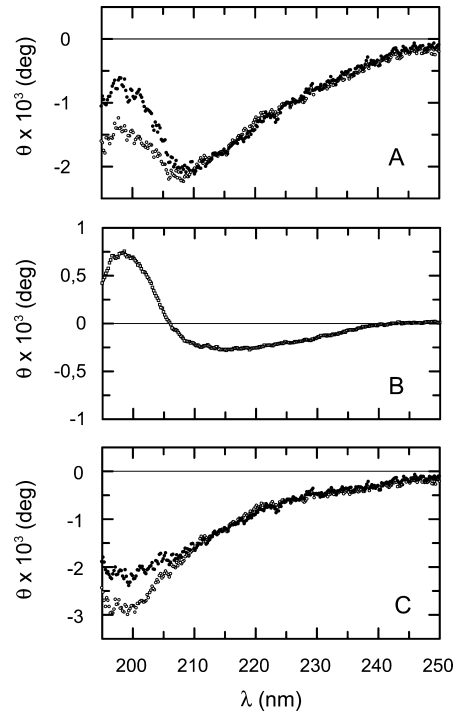

FIGURE 5: Far-UV CD spectra of E1 (201–432) with three disulfide bonds [C(13)−C(14), C(17)−C(18), and C(19)−C(20)] in comparison with the cysteine-free E1 variant. (A) Overlay of the spectra of 1.5 μM SlyD*−SlyD*−E1 with three disulfide bonds (●) and without cysteine residues (○) in 10 mM potassium phosphate and 100 mM KF. (B) Spectrum of 1.5 M SlyD*−SlyD* in the same buffer. (C) The signal contribution of the chaperone module, SlyD*−SlyD*, was subtracted from the spectra of both E1 fusion proteins. The resulting ellipticity is given in degrees.

that combine an optimal solubility with an excellent antigenicity. They can be obtained in large quantities from an *E. coli* host and refolded to a nativelike conformation in a simple and reproducible manner.

Role of the Fused Chaperone Modules in the Solubility of the E1 Fragment. After having optimized the C-terminal fragment with respect to length and disulfide bonding, we examined whether the covalent fusion with two SlyD* modules is still required to keep this protein in its soluble functional form. Toward this end, three E1 variants were compared, without SlyD*, and with one or two SlyD* modules fused to their N-termini. When renatured under unfavorable conditions, these three variants differed strongly in their tendency to aggregate (Figure 6A). In the absence of SlyD*, the protein aggregated markedly at 35 °C, and the level of aggregation was reduced in the presence of one SlyD* module and almost completely suppressed when both SlyD* modules were present. Virtually identical results were found when FkpA was used as a fusion partner for the E1 ectodomain variants (P. Schaarschmidt and C. Scholz, unpublished results). The suppression of E1 aggregation was less efficient when SlyD* was added to the refolding buffer in *trans*. The aggregation of 0.1 μM E1 ectodomain was only partially suppressed by 1 μM SlyD* (Figure 6B). The covalent linkage increases the effective concentration of the chaperone in the proximity of the substrate protein, and this explains why covalently linked SlyD* is such an excellent folding helper.

SlyD* not only assists the matrix-coupled refolding process but also improves the long-term solubility (i.e., the

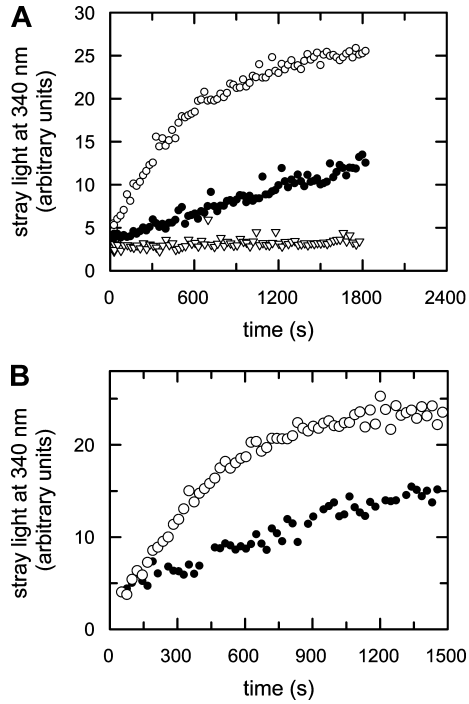

FIGURE 6: Influence of SlyD* and SlyD*−SlyD* fusion modules on the aggregation of denatured Rubella E1 (201–432) at 35 °C. Unfolded E1 (201–432) [in 6.0 M GdmCl, 20 mM DTT, and 50 mM potassium phosphate (pH 7.0)] was diluted to a final concentration of 0.1 μM in 50 mM potassium phosphate (pH 7.0), 44 mM GdmCl, 100 mM KCl, and 20 mM DTT. (A) The kinetics of aggregation as monitored by the increase in light scattering at 340 nm were followed for E1 without a fusion partner (○), SlyD*−E1 (●), and SlyD*−SlyD*−E1 (▽). (B) Kinetics of aggregation of 0.1 μM E1 (201–432) in the absence (○) and presence (●) of 1.0 μM SlyD*.

shelf life) of aggregation-prone client proteins. Indeed, the solubilization of Rubella E1 (201–432) by tandem SlyD* is efficient enough to extend the shelf life of the E1 antigenicity to several months. The results for the E1 ectodomain resemble those obtained previously with the gp41, gp36, and gp21 ectodomains from HIV-1, HIV-2, and HTLV, respectively. All these hydrophobic proteins were efficiently solubilized by tandem fusion with chaperone proteins and exhibited very high immunological reactivity (*39*).

DISCUSSION

Rubella virus infects its human host via endocytosis and an acid-triggered fusion step. The envelope protein E1 plays a dominant role in membrane fusion (*6*), which requires flexibility and large conformational rearrangements within the ectodomains of Rubella (*57*) and other viruses (*58*). The disulfide bonds of the E1 ectodomain are essential, and reduction of Rubella virions by mercaptoethanol abolishes hemagglutination and compromises infectivity (*59*).

E1 is the major target of the humoral immune response, and variants or fragments of E1 are routinely employed in serological assays for detection of anti-Rubella immunoglobulins. The recombinant production of the E1 ectodomain in a prokaryotic host and in vitro refolding are complicated by its conformational flexibility, the need to form 10 disulfide bonds, and the presence of hydrophobic stretches such as the fusion peptide (*6, 7*).

Here, we linked various fragments of the Rubella E1 ectodomain with a tandem SlyD* repeat and produced the corresponding fusion proteins in *E. coli*. SlyD* is an energy-independent chaperone and suppresses protein aggregation by binding reversibly to folding intermediates, probably via its IF (insert in flap) domain (*46*). Its overproduction is tolerated well in the *E. coli* cytosol (*39, 42*). The fusion polypeptides were produced in large amounts and formed inclusion bodies. Several of these could be refolded in vitro to a highly soluble form with very high antigenicity.

E1 (201–432) fragments in fusion with two SlyD* modules and with two disulfide bonds, either C(17)−C(18) and C(19)−C(20) bonds or C(13)−C(14) and C(17)−C(18) bonds, exhibited excellent solubility, reactivity, and selectivity. Since they can easily be produced at high yields in *E. coli*, they will be invaluable tools for the specific and sensitive detection of anti-Rubella IgG in immunoassays. The disulfides are essential for the function, and the replacement of the corresponding Cys residues with Ala largely abolished IgG binding. This agrees with earlier reports about the importance of disulfide bonds for E1 antigenicity (*32, 59, 60*).

Addition of the single C(13)−C(14) disulfide bond led to significant immunological reactivity of fragment 201–432 (Table 2). This finding is in line with reports about peptide BCH-178, which encompasses the E1 neutralizing epitope 213–239 with the C(13)−C(14) disulfide bond (*36*). BCH-178 has been ascribed a high predictive capacity for Rubella immunity, and it has been used as a peptide antigen in ELISA serology (*35, 36*). Unlike other neutralizing epitopes (*61*), it is highly conserved among all known Rubella virus strains (*38, 62*). Wolinsky and co-workers assigned the neutralizing epitope within BCH-178 to residues 221–239 and 223–239 (*63*), which encompass the C(13)−C(14) disulfide bond. The substitution of cysteine residues 225 (C13) and 235 (C14) with α-aminobutyrate abrogated IgG binding (*32*). The reactivity of our E1 (201–432) fragment with the single C(13)−C(14) disulfide bond was modest and not sufficient for the development of a robust and sensitive anti-Rubella DAGS immunoassay (Table 2). The antigenicity of this fragment could, however, be strongly increased via addition of the C(17)−C(18) disulfide bond (Table 3). Similarly, the double-disulfide variant, C(17)−C(18)/C(19)−C(20), exhibited a very high immunoreactivity.

The N-terminal half of Rubella E1 is not suited for the detection of anti-Rubella antibodies. N-Terminal fragments with or without disulfide bonds were soluble, but the immunological reactivities were poor. It has been suggested that the N-terminal part of E1 mediates membrane fusion, whereas the C-terminal part is important for E1 oligomerization. The hydrophobic region encompassing amino acids 81–109 has been attributed the role of a fusion peptide (*6, 7*). This part of E1 is probably inaccessible in the prefusogenic state to prevent aggregation of virus particles, which might explain why the entire N-terminal region is less immunogenic and why all neutralizing epitopes have been found to cluster in the C-terminal half of the E1 ectodomain (*32, 36, 55, 63–65*).

The E1 fusion construct with optimal antigenicity identified in this study [E1 (201–432)] encompasses all four known neutralizing epitopes that have been localized in the region of residues 202–285. Antibodies that react with these epitopes are correlated with immunity and thus are of prime importance in Rubella immunodiagnostics. Because of its ease of production and handling, its high solubility, and its excellent binding to anti-E1 IgG, the engineered SlyD*−SlyD*−E1

(201–432) fusion polypeptide will be very useful for monitoring the immune status in Rubella serology.

The chaperone−E1 fusion proteins formed inclusion bodies in the *E. coli* cytosol, indicating that the SlyD* modules could not prevent aggregation during protein overexpression in vivo. After solubilization and unfolding by a denaturant, however, SlyD* mediated the in vitro refolding of the E1 ectodomain fragments very efficiently. Matrix-assisted refolding was well suited to renaturation of the ectodomain fusion proteins, to ensuring formation of the correct disulfide bonds, and finally to reaching a yield of ~5 mg of nativelike E1/g of cell wet weight. The nativelike conformation of the E1 fragment attained in the refolded fusion protein is corroborated by its excellent immunoreactivity in a DAGS assay based on the automated Elecsys analyzer system (Roche Diagnostics).

Binding to a solid support increased the yield of several other reactivated proteins (*66, 67*). The covalently fused chaperones assist refolding probably by shielding hydrophobic patches in folding intermediates. Since they are covalently fixed to the folding target via a long and flexible linker, the effective concentration of SlyD* is kept high during folding. It is puzzling that a single SlyD* unit is not sufficient to keep E1 soluble for an extended period of time. The SlyD*−E1 protein still aggregates, albeit very slowly, whereas the SlyD*−SlyD*−E1 protein remains a soluble monomer even under unfavorable conditions such as high concentrations (>10 mg/mL) and elevated temperatures (>40 °C). Obviously, the SlyD*−SlyD* tandem fusion partner significantly prolongs the shelf life of a hydrophobic protein such as E1 without hampering its antigenicity. Thus, the affinity of the SlyD*−SlyD* fusion module for the E1 part is well balanced to combine two apparently opposite functions. On one hand, the affinity between the chaperone and E1 is sufficiently high to warrant the formation of a soluble complex. On the other hand, the affinity is sufficiently low to allow immunoglobulins to access and bind to E1 epitopes. Possibly, these two requirements are met for the SlyD*−SlyD*−E1 protein because it exists in a dynamic equilibrium between a closed form and an open form.

There are several strategies for the recombinant production of difficult target proteins in *E. coli* (*68, 69*). Cysteine-rich or toxic proteins are usually directed to the periplasm via a fused export signal sequence (*70*). We produced the engineered E1 fragments in the *E. coli* cytoplasm and developed an efficient refolding and reoxidation protocol for the resulting fusion proteins with two SlyD* modules. Fusion tags are often cleaved off after purification to produce the mature target protein. Here, the fused chaperone modules remain covalently linked to their client protein. This might be particularly advantageous for viral envelope proteins such as Rubella E1, which are naturally produced as polyprotein precursors. SlyD possibly restores in part the benign solubility properties of the polypeptide precursor without compromising the immunological reactivity of the mature protein. As fusion partners, SlyD and FkpA also improved the solubility and immunoreactivity of the envelope proteins gp41 from HIV-1, gp36 from HIV-2, and gp21 from HTLV (*39*). Very recently, another report on the outstanding solubilization properties of SlyD highlighted the potential of this molecule in biotechnological applications (*71*). We suggest that the fusion of a protein with one or two modules of SlyD* or related PPIase chaperones, overproduction as insoluble inclusion bodies, and in vitro refolding provide a good strategy for producing difficult proteins of diagnostic or therapeutic value in a functional form.

ACKNOWLEDGMENT

This work was performed in the DXR-IR, DXR-IH, and DXR-RE departments of Roche Diagnostics GmbH (Penzberg, Germany). The excellent technical assistance of Franz Wagner, Nicole Amtmann, Achim Gärtner, Brigitta Richter, Petra Bierth, and Sima-Hassanzadeh-Makooi is gratefully acknowledged. We thank Manfred Ginter, Silvia Entenmann, and Andrea Oenings for performing the Elecsys measurements and Helmut Lenz, Klaus Hirzel, Herbert Andres, and Gabriele Pestlin for helpful comments on the manuscript. I dedicate this manuscript to my parents, Wolfgang and Christine Scholz, on the occasion of their 40th wedding anniversary.

REFERENCES

1. Wolinsky, J. S. (1988) Teratogenic and Delayed Consequences of Maternal Rubella. *Teratology 37*, 516–516.
2. Reef, S. E., Frey, T. K., Theall, K., Abernathy, E., Burnett, C. L., Icenogle, J., McCauley, M. M., and Wharton, M. (2002) The changing epidemiology of Rubella in the 1990s: On the verge of elimination and new challenges for control and prevention. *J. Am. Med. Assoc. 287*, 464–472.
3. Parkman, P. D. (1999) Making vaccination policy: The experience with Rubella. *Clin. Infect. Dis. 28* (Suppl. 2), 140–146.
4. Oker-Blom, C. (1984) The Gene Order for Rubella Virus Structural Proteins is NH2-C-E2-E1-COOH. *J. Virol. 51*, 354–358.
5. Oker-Blom, C., Jarvis, D. L., and Summers, M. D. (1990) Translocation and Cleavage of Rubella Virus Envelope Glycoproteins: Identification and Role of the E2 Signal Sequence. *J. Gen. Virol. 71*, 3047–3053.
6. Yang, D. C., Hwang, D., Qiu, Z. Y., and Gillam, S. (1998) Effects of mutations in the Rubella virus E1 glycoprotein on E1-E2 interaction and membrane fusion activity. *J. Virol. 72*, 8747–8755.
7. Qiu, Z. Y., Yao, J. S., Cao, H. W., and Gillam, S. (2000) Mutations in the E1 hydrophobic domain of Rubella virus impair virus infectivity but not virus assembly. *J. Virol. 74*, 6637–6642.
8. Waxham, M. N., and Wolinsky, J. S. (1983) Immunochemical identification of Rubella virus hemagglutinin. *Virology 126*, 194–203.
9. Baron, M. D., and Forsell, K. (1991) Oligomerization of the Structural Proteins of Rubella Virus. *Virology 185*, 811–819.
10. de Mazancourt, A., Waxham, M. N., Nicolas, J. C., and Wolinsky, J. S. (1986) Antibody Response to the Rubella Virus Structural Proteins in Infants with the Congenital Rubella Syndrome. *J. Med. Virol. 19*, 111–122.
11. Zhang, T., Mauracher, C. A., Mitchell, L. A., and Tingle, A. J. (1992) Detection of Rubella Virus Specific Immunoglobulin G (IgG), IgM, and IgA Antibodies by Immunoblot Assays. *J. Clin. Microbiol. 30*, 824–830.
12. Katow, S., and Sugiura, A. (1985) Antibody Response to Individual Rubella Virus Proteins in Congenital and Other Rubella Virus Infections. *J. Clin. Microbiol. 21*, 449–451.
13. Chaye, H. H., Mauracher, C. A., Tingle, A. J., and Gillam, S. (1992) Cellular and Humoral Immune Responses to Rubella Virus Structural Protein E1, Protein E2, and Protein C. *J. Clin. Microbiol. 30*, 2323–2329.
14. Vaheri, A., Sedwick, W. D., Plotkin, S. A., and Maes, R. (1965) Cytopathic effect of Rubella virus in BHK21 cells and growth to high titers in suspension cuture. *Virology 27*, 239–241.
15. Bardeletti, G., Kessler, N., and Aymard-Henry, M. (1975) Morphology, biochemical analysis and neuraminidase activity of rubella virus. *Arch. Virol. 49*, 175–186.
16. Hobman, T. C., Seto, N. O. L., and Gillam, S. (1994) Expression of Soluble Forms of Rubella Virus Glycoproteins in Mammalian Cells. *Virus Res. 31*, 277–289.

17. Seto, N. O. L., and Gillam, S. (1994) Expression and Characterization of a Soluble Rubella Virus E1 Envelope Protein. *J. Med. Virol. 44*, 192–199.
18. Seppänen, H., Huhtala, M. L., Vaheri, A., Summers, M. D., and Oker-Blom, C. (1991) Diagnostic Potential of Baculovirus-Expressed Rubella Virus Envelope Proteins. *J. Clin. Microbiol. 29*, 1877–1882.
19. Oker-Blom, C., Pettersson, R. F., and Summers, M. D. (1989) Baculovirus Polyhedrin Promoter-Directed Expression of Rubella Virus Envelope Glycoprotein E1 and Glycoprotein E2, in *Spodoptera frugiperda* Cells. *Virology 172*, 82–91.
20. Perrenoud, G., Messerli, E., Thierry, A. C., Beltraminelli, N., Cousin, P., Fasel, N., Vallet, V., Demotz, S., Duchosal, M. A., and Moulon, C. (2004) A recombinant Rubella virus E1 glycoprotein as a rubella vaccine candidate. *Vaccine 23*, 480–488.
21. Wen, H. L., and Wang, Z. Y. (2005) Expression and characterization of Rubella virus glycoprotein E1 in yeast cells. *Intervirology 48*, 321–328.
22. Grangeot-Keros, L., Pustowoit, B., and Hobman, T. (1995) Evaluation of Cobas Core Rubella IgG EIA recomb, a New Enzyme Immunoassay Based on Recombinant Rubella-Like Particles. *J. Clin. Microbiol. 33*, 2392–2394.
23. Qiu, Z. Y., Ou, D. W., Wu, H., Hobman, T. C., and Gillam, S. (1994) Expression and Characterization of Virus-Like Particles Containing Rubella Virus Structural Proteins. *J. Virol. 68*, 4086–4091.
24. Giessauf, A., Flaim, M., Dierich, M. P., and Würzner, R. (2002) A technique for isolation of Rubella virus-like particles by sucrose gradient ultracentrifugation using Coomassie Brilliant Blue G crystals. *Anal. Biochem. 308*, 232–238.
25. Gros, C., Linder, M., Wengler, G., and Wengler, G. (1997) Analyses of disulfides present in the Rubella virus E1 glycoprotein. *Virology 230*, 179–186.
26. Ho-Terry, L., and Cohen, A. (1984) The role of glycosylation on haemagglutination and immunological reactivity of Rubella virus. *Arch. Virol. 79*, 139–146.
27. Qiu, Z. Y., Tufaro, F., and Gillam, S. (1992) The Influence of N-Linked Glycosylation on the Antigenicity and Immunogenicity of Rubella Virus E1 Glycoprotein. *Virology 190*, 876–881.
28. Hobman, T. C., Qiu, Z. Y., Chaye, H., and Gillam, S. (1991) Analysis of Rubella Virus E1 Glycosylation Mutants Expressed in COS Cells. *Virology 181*, 768–772.
29. Terry, G. M., Ho-Terry, L., Londesborough, P., and Rees, K. R. (1989) A Bio-Engineered Rubella E1 Antigen. *Arch. Virol. 104*, 63–75.
30. Newcombe, J., Starkey, W., Al-Mumin, S., Knight, A. I., Best, J. M., and Sanders, P. G. (1994) Recombinant Rubella E1 fusion proteins for antibody screening and diagnosis. *Clin. Diagn. Virol. 2*, 149–163.
31. Starkey, W. G., Newcombe, J., Corbett, K. M., Liu, K. M., Sanders, P. G., and Best, J. M. (1995) Use of Rubella Virus E1 Fusion Proteins for Detection of Rubella Virus Antibodies. *J. Clin. Microbiol. 33*, 270–274.
32. Wolinsky, J. S., McCarthy, M., Allencannady, O., Moore, W. T., Jin, R., Cao, S. N., Lovett, A., and Simmons, D. (1991) Monoclonal Antibody-Defined Epitope Map of Expressed Rubella Virus Protein Domains. *J. Virol. 65*, 3986–3994.
33. Mitchell, L. A., Décarie, D., Tingle, A. J., Zrein, M., and Lacroix, M. (1993) Identification of Immunoreactive Regions of Rubella Virus E1 and Virus E2 Envelope Proteins by Using Synthetic Peptides. *Virus Res. 29*, 33–57.
34. Chaye, H., Ou, D. W., Chong, P. L., and Gillam, S. (1993) Human T-Cell and B-Cell Epitopes of E1 Glycoprotein of Rubella Virus. *J. Clin. Immunol. 13*, 93–100.
35. Giessauf, A., Letschka, T., Walder, G., Dierich, M. P., and Würzner, R. (2004) A synthetic peptide ELISA for the screening of rubella virus neutralizing antibodies in order to ascertain immunity. *J. Immunol. Methods 287*, 1–11.
36. Mitchell, L. A., Zhang, T., Ho, M., Décarie, D., Tingle, A. J., Zrein, M., and Lacroix, M. (1992) Characterization of Rubella Virus-Specific Antibody Responses by Using a New Synthetic Peptide-Based Enzyme-Linked-Immunosorbent-Assay. *J. Clin. Microbiol. 30*, 1841–1847.
37. Pustowoit, B., and Liebert, U. G. (1998) Predictive value of serological tests in Rubella virus infection during pregnancy. *Intervirology 41*, 170–177.
38. Zrein, M., Joncas, J. H., Pedneault, L., Robillard, L., Dwyer, R. J., and Lacroix, M. (1993) Comparison of a Whole Virus Enzyme Immunoassay (EIA) with a Peptide-Based EIA for Detecting Rubella Virus Immunoglobulin G Antibodies Following Rubella Vaccination. *J. Clin. Microbiol. 31*, 1521–1524.
39. Scholz, C., Schaarschmidt, P., Engel, A. M., Andres, H., Schmitt, U., Faatz, E., Balbach, J., and Schmid, F. X. (2005) Functional solubilization of aggregation-prone HIV envelope proteins by covalent fusion with chaperone modules. *J. Mol. Biol. 345*, 1229–1241.
40. Hottenrott, S., Schumann, T., Plückthun, A., Fischer, G., and Rahfeld, J. U. (1997) The *Escherichia coli* SlyD is a metal ion-regulated peptidyl-prolyl cis/trans-isomerase. *J. Biol. Chem. 272*, 15697–15701.
41. Zhang, J. W., Butland, G., Greenblatt, J. F., Emili, A., and Zamble, D. B. (2005) A role for SlyD in the *Escherichia coli* hydrogenase biosynthetic pathway. *J. Biol. Chem. 280*, 4360–4366.
42. Scholz, C., Eckert, B., Hagn, F., Schaarschmidt, P., Balbach, J., and Schmid, F. X. (2006) SlyD proteins from different species exhibit high prolyl isomerase and chaperone activities. *Biochemistry 45*, 20–33.
43. Ramm, K., and Plückthun, A. (2001) High enzymatic activity and chaperone function are mechanistically related features of the dimeric *E. coli* peptidyl-prolyl isomerase FkpA. *J. Mol. Biol. 310*, 485–498.
44. Arié, J. P., Sassoon, N., and Betton, J. M. (2001) Chaperone function of FkpA, a heat shock prolyl isomerase, in the periplasm of *Escherichia coli*. *Mol. Microbiol. 39*, 199–210.
45. Saul, F. A., Arié, J. P., Normand, B. V. L., Kahn, R., Betton, J. M., and Bentley, G. A. (2004) Structural and functional studies of FkpA from *Escherichia coli*, a cis/trans peptidyl-prolyl isomerase with chaperone activity. *J. Mol. Biol. 335*, 595–608.
46. Knappe, T. A., Eckert, B., Schaarschmidt, P., Scholz, C., and Schmid, F. X. (2007) Insertion of a chaperone domain converts FKBP12 into a powerful catalyst of protein folding. *J. Mol. Biol. 368*, 1458–1468.
47. Dominguez, G., Wang, C. Y., and Frey, T. K. (1990) Sequence of the Genome RNA of Rubella-Virus: Evidence for Genetic Rearrangement During Togavirus Evolution. *Virology 177*, 225–238.
48. Schägger, H., and von Jagow, G. (1987) Tricine Sodium Dodecyl-Sulfate Polyacrylamide-Gel Electrophoresis for the Separation of Proteins in the Range from 1 kDa to 100 kDa. *Anal. Biochem. 166*, 368–379.
49. Pace, C. N., Vajdos, F., Fee, L., Grimsley, G., and Gray, T. (1995) How to Measure and Predict the Molar Absorption Coefficient of a Protein. *Protein Sci. 4*, 2411–2423.
50. Buchner, J., Grallert, H., and Jakob, U. (1998) Analysis of chaperone function using citrate synthase as nonnative substrate protein. *Methods Enzymol. 290*, 323–338.
51. Volkin, D. B., Mach, H., and Middaugh, C. R. (1997) Degradative covalent reactions important to protein stability. *Mol. Biotechnol. 8*, 105–122.
52. Eisenberg, D., Schwarz, E., Komaromy, M., and Wall, R. (1984) Analysis of Membrane and Surface Protein Sequences with the Hydrophobic Moment Plot. *J. Mol. Biol. 179*, 125–142.
53. Kyte, J., and Doolittle, R. F. (1982) A Simple Method for Displaying the Hydropathic Character of a Protein. *J. Mol. Biol. 157*, 105–132.
54. Sedlak, J., and Raymond, H. L. (1968) Estimation of Total, Protein-Bound, and Nonprotein Sulfhydryl Groups in Tissue with Ellman's Reagent. *Anal. Biochem. 25*, 192–205.
55. Terry, G. M., Ho-Terry, L., Londesborough, P., and Rees, K. R. (1988) Localization of the Rubella E1 Epitopes. *Arch. Virol. 98*, 189–197.
56. Huber-Wunderlich, M., and Glockshuber, R. (1998) A single dipeptide sequence modulates the redox properties of a whole enzyme family. *Folding Des. 3*, 161–171.
57. Katow, S., and Sugiura, A. (1988) Low pH-Induced Conformational Change of Rubella Virus Envelope Proteins. *J. Gen. Virol. 69*, 2797–2807.
58. Weissenhorn, W., Dessen, A., Calder, L. J., Harrison, S. C., Skehel, J. J., and Wiley, D. C. (1999) Structural basis for membrane fusion by enveloped viruses. *Mol. Membr. Biol. 16*, 3–9.
59. Ho-Terry, L., and Cohen, A. (1981) Effect of 2-mercaptoethanol on the haemagglutinating activity and antigenic properties of Rubella virus. *Arch. Virol. 70*, 199–206.
60. Green, K. Y., and Dorsett, P. H. (1986) Rubella Virus Antigens: Localization of Epitopes Involved in Hemagglutination and Neutralization by Using Monoclonal Antibodies. *J. Virol. 57*, 893–898.

61. Londesborough, P., Ho-Terry, L., and Terry, G. (1995) Sequence Variation and Biological Activity of Rubella Virus Isolates. *Arch. Virol. 140*, 563–570.
62. Frey, T. K., Abernaty, E. S., Bosma, T. J., Starkey, W. G., Corbett, K. M., Best, J. M., Katow, S., and Weaver, S. C. (1998) Molecular analysis of rubella virus epidemiology across three continents, North America, Europe, and Asia, 1961–1997. *J. Infect. Dis. 178*, 642–650.
63. Wolinsky, J. S., Sukholutsky, E., Moore, W. T., Lovett, A., McCarthy, M., and Adame, B. (1993) An Antibody Peptide-Defined and Synthetic Peptide-Defined Rubella Virus E1 Glycoprotein Neutralization Domain. *J. Virol. 67*, 961–968.
64. Ho-Terry, L., Terry, G. M., Cohen, A., and Londesborough, P. (1986) Immunological characterization of the Rubella E1 glycoprotein. Brief report. *Arch. Virol. 90*, 145–152.
65. Chaye, H., Chong, P., Tripet, B., Brush, B., and Gillam, S. (1992) Localization of the Virus Neutralizing and Hemagglutinin Epitopes of E1 Glycoprotein of Rubella Virus. *Virology 189*, 483–492.
66. Stempfer, G., Höll-Neugebauer, B., and Rudolph, R. (1996) Improved refolding of an immobilized fusion protein. *Nat. Biotechnol. 14*, 329–334.
67. Lilie, H., Schwarz, E., and Rudolph, R. (1998) Advances in refolding of proteins produced in *E. coli*. *Curr. Opin. Biotechnol. 9*, 497–501.
68. Baneyx, F., and Mujacic, M. (2004) Recombinant protein folding and misfolding in *Escherichia coli*. *Nat. Biotechnol. 22*, 1399–1408.
69. Georgiou, G., and Segatori, L. (2005) Preparative expression of secreted proteins in bacteria: Status report and future prospects. *Curr. Opin. Biotechnol. 16*, 538–545.
70. Mergulhao, F. J. M., Summers, D. K., and Monteiro, G. A. (2005) Recombinant protein secretion in *Escherichia coli*. *Biotechnol. Adv. 23*, 177–202.
71. Han, K. Y., Song, J. A., Ahn, K. Y., Park, J. S., Seo, H. S., and Lee, J. (2007) Solubilization of aggregation-prone heterologous proteins by covalent fusion of stress-responsive *Escherichia coli* protein, SlyD. *Protein Eng. Des. Sel. 20*, 543–549.

BI702435V